

Flying-seed-like liquid crystals 5[†]: Liquid crystals based on octakisphenylthiophthalocyanine and their optical properties

Aya Ishikawa,^a Kazuchika Ohta*^a and Mikio Yasutake^b

^aSmart Material Science and Technology, Interdisciplinary Graduate School of Science and Technology, Shinshu University, 1-15-1 Tokida, Ueda, 386-8567, Japan.

^bComprehensive Analysis Center for Science, Saitama University, 255 Shimo-okubo, Sakura-ku, Saitama 338-8570, Japan.

Received date (to be automatically inserted after your manuscript is submitted)

Accepted date (to be automatically inserted after your manuscript is accepted)

ABSTRACT: We have synthesized three novel flying-seed-like liquid crystals based on phthalocyaninato copper(II) (abbreviated as PcCu) substituted by bulky groups $\{(o-C_1)PhS$ (**i**), $(m-C_1)PhS$ (**j**), $[m,p-(C_1)_2]PhS$ (**k**) instead of using long alkyl chains, in order to investigate their mesomorphism. Their phase transition behaviour and the mesophase structures have been established by using a polarizing optical microscope, a differential scanning calorimeter, and a temperature-dependent small angle X-ray diffractometer. As the results, $[(o-C_1)PhS]_8PcCu$ (**8i**), $[(m-C_1)PhS]_8PcCu$ (**8j**) and $\{[m,p-(C_1)_2]PhS\}_8PcCu$ (**8k**) show a $Col_{tet,o}$ mesophase at 314.9 ~ 362.9°C, a $Col_{ro}(P2m)$ mesophase at 287.4 ~ 334.2°C and a $Col_{ro}(P2m)$ mesophase at 331.8 ~ 386.8°C, respectively. Very interestingly, each of the derivatives thus exhibits a columnar mesophase at very high temperatures. The mesomorphism is apparently originated from the novel bulky groups (**i**~**k**). It is also noteworthy that the Q bands of the present PhS-containing Pc derivatives **8i**~**k** in THF significantly red-shift by about 35nm in comparison with those of the corresponding PhO-containing derivatives in THF.

KEYWORDS: flying-seed-like liquid crystals, metallomesogen, phthalocyanine, columnar mesophase.

*Correspondence to: Smart Material Science and Technology, Interdisciplinary Graduate School of Science and Technology, Shinshu University, 1-15-1 Tokida, Ueda, 386-8567, Japan. E-mail: ko52517@shinshu-u.ac.jp; Fax: +81-268-21-5492; Tel: +81-268-21-5492

†Part 4: ref. 17 in this paper.

INTRODUCTION

Liquid crystals are intermediate phases between liquid and crystal as the name suggests, and they have both flexibility of liquid and molecular orientational order of crystal. From this unique fascinating nature, many liquid crystals have been synthesized since the first liquid crystals were discovered by Reinitzer in 1888 [1, 2]. Liquid crystals may be originated from orientational order of the rigid central core parts and fluidity of the molten peripheral long alkyl chains. Therefore, they can show both characteristics of liquid and crystal. Almost all the liquid-crystalline materials know up to date can be broadly categorized into two groups of calamitic liquid crystals and discotic liquid crystals. The first group of calamitic liquid crystals has a rod-like molecular shape, whereas the second group of discotic liquid crystals found by Chandrasekhar et al in 1977 [3] has a disk-like molecular shape. Both groups of the liquid crystals commonly have long alkyl chains in periphery and a flat central core. Accordingly, people have long believed that liquid crystals should have both a rigid central core and flexible peripheral alkyl chains. However, a very few liquid crystals being out of this common sense have been reported [4-12].

In 1910 Vorländer reported that potassium dimethylacetate ($(\text{CH}_3)_2\text{CHCOOK}$: **1** in Fig. 1[A]), potassium diethylacetate ($(\text{C}_2\text{H}_5)_2\text{CHCOOK}$: **2**) and sodium diphenylacetate ($\text{Ph}_2\text{CHCOONa}$: **3**) show liquid crystalline property (= mesomorphism)[4]. These alkali metal carboxylates have neither a rigid central core nor flexible peripheral long alkyl chains, but each of them shows mesomorphism. They are very far from general concept of liquid crystals and show mesophases only at very high temperatures. Accordingly, these liquid crystals have seldom been investigated in detail for about 100 years.

In 2006, we revealed by using temperature-dependent X-ray diffraction technique that both $(\text{CH}_3)_2\text{CHCOOK}$ (**1**) and $(\text{C}_2\text{H}_5)_2\text{CHCOOK}$ (**2**) show a smectic A (SmA) mesophase and $\text{Ph}_2\text{CHCOONa}$ (**3**) shows a hexagonal columnar (Col_h) mesophase [9]. Since these liquid crystalline materials resemble flying-seeds like as a maple seed, this type of liquid crystals is named as “**flying-seed-like liquid crystals**”. They are the third type of liquid crystals different from calamitic and discotic liquid crystals. These flying-seed-like liquid crystals may show mesomorphism by free rotation of the bulky substituents to form soft parts instead of long alkyl chains [9]. As far as we know, the other alkali metal carboxylates having no long alkyl chains have been studied until now by a very few researchers: Demus *et al.* in 1970[5], Sanesi *et al.* in 1978 [6, 7] and Binnemans *et al.* in 2005[8].

In 2009, Usol'tseva and her co-workers found from polarizing optical microscopic observations that a phthalocyanine (Pc) derivative substituted by four triphenylmethyl groups, $(3\text{Ph-PhO})_4\text{PcCu}$ (**4a**), depicted in Fig. 1[B] shows a mesophase[13,14]. The substituent of triphenylmethyl group in this compound very resembles the molecular structure of $\text{Ph}_2\text{CHCOONa}$ (**3**) in Fig. 1[A]. Therefore, we thought that this Pc derivative might be one of the flying-seed-like liquid crystals induced by free rotation of the peripheral bulky substituents. In 2012, we carried out temperature-dependent X-ray diffraction studies on these Pc derivatives **4a-d** and revealed that they show columnar mesophases [15]. Recently, we reported that introduction of the bulky substituents to the other cores also induce a nematic mesophase for Compound **5d** in Fig. 1[C] and a rectangular columnar mesophase for Compounds **6b** and **6d** in Fig. 1[D] [16].

Furthermore, we have revealed for novel flying-seed-like Pc compounds **7e-h** in Fig. 1[E] that their mesomorphism is originated from flip-flop of bulky substituents and greatly depend on the substitution position of methoxy group [17]. In these compounds, two adjacent phenoxy groups cannot freely rotate but flip-flop within the restricted angles. However, when this phenoxy group is further substituted by (a) methoxy group(s) at the *o*, *m*, *p* positions, the resulting bulkier phenoxy group originates bigger excluded volume for the derivatives by the flip-flop. Accordingly, mesomorphism may be also induced not only by free rotation but also by flip-flop of bulky substituents. As the results, $[(o\text{-C}_1)\text{PhO}]_8\text{PcCu}$ (**7e**) shows a monotropic $\text{Col}_{r_0}(\text{P2m})$ mesophase; $[(m\text{-C}_1)\text{PhO}]_8\text{PcCu}$ (**7f**) and $\{[m,p-$

(C₁)₂[PhO]₈PcCu (**7h**) show enantiotropic columnar mesophases of Col_{ro}(P2₁/a), whereas [(*p*-C₁)PhO]₈PcCu (**7g**) show no mesophase. Thus, the derivative (**7g**) substituted by a methoxy group at a *para* position does not show mesomorphism, because the excluded volume originated by the flip-flopping substituent is small. On the other hand, the derivatives substituted by (a) methoxy group(s) at (a) *meta* position(s) (**7f** and **7h**) show enantiotropic mesomorphism, because the excluded volume is big enough. The derivative (**7e**) substituted by a methoxy group at an *ortho* position shows monotropic mesomorphism, because the excluded volume is big enough but the steric hindrance may block the stacking the central Pc cores. Thus, we could successfully induce their mesomorphism by using a novel series of bulky substituents. These novel mesophase-inducing groups (**e**, **f** and **h**) are more advantageous in synthesis of flying-seed-like liquid crystals than the previous mesophase-inducing groups (**a**~**d**), because the synthesis becomes much easier. The target compounds **7e**~**g** could be prepared in only two steps from the starting material.

If this new type of flying-seed-like liquid crystals may additionally exhibit fast charge mobility, we can easily obtain donor semiconductor liquid crystals at very high temperatures. They may extremely improve thermal stability of organic thin film solar cells. Phenylthio group may possess a band gap of the HOMO-LUMO narrower than that of phenoxy group, so that the charge carrier mobility may be improved. It can be deduced from the analogy between the Pc derivatives substituted by alkylthio group and/or alkoxy group [18]. The charge carrier mobility of the alkylthio-substituted liquid crystal, (C₁₂S)₈PcH₂, is 5 times higher than that of the alkoxy-substituted liquid crystal, (C₁₂O)₈PcH₂ [19]. Therefore we can expect that if novel phenylthio-substituted Pc liquid crystals could be synthesized, they would show very fast charge carrier mobilities.

In this study, we have synthesized three novel flying-seed-like liquid crystals based on octaphenylthiophthalocyaninato copper(II) (abbreviated as (PhS)₈PcCu) in which each of the phenylthio group is further substituted by (a) methoxy group(s) at the *o*, *m*, *p* positions, in order to investigate the mesomorphism and electronic spectral properties. Up to date a few derivatives based on (PhS)₈PcCu have been reported [20, 21], and there have never been reports of the mesomorphism. We believe that this study may contribute to further develop the field of flying-seed-like liquid crystals which is still in infancy.

EXPERIMENTAL

Synthesis

In Scheme 1 is shown synthetic route for novel flying-seed-like liquid crystals based on (PhS)₈PcCu. The starting materials of 4,5-dichlorophthalonitrile, *o*-methoxythiophenol (**9i**), *m*-methoxythiophenol (**9j**) and *m,p*-dimethoxythiophenol (**9k**) were purchased from Tokyo Kasei. The phthalonitrile derivatives (**10i**~**k**) were prepared by the method of Wöhrle *et al* [22]. Each of the final (PhS)₈PcCu derivatives (**8i**~**k**) was synthesized by cyclic tetramerization of the phthalonitrile derivatives (**10i**~**k**). The detailed synthetic procedures are described below only for the representative phthalocyanine derivative, [(*m*-C₁)PhS]₈PcCu (**8j**). For the other phthalocyanine derivatives (**8i** and **8k**) and the precursors (**10i** and **10k**), their physical properties are only described.

4,5-Bis(3-methoxyphenylthio)phthalonitrile (10j)

A mixture of *o*-methoxythiophenol (**9j**: 0.372 g, 2.65 mmol), dry DMSO (8 ml) and K₂CO₃ (3.02 g, 21.9 mmol) was heated at 90°C for 15min with stirring under nitrogen atmosphere. Then, to this reaction mixture was added 4,5-dichlorophthalonitrile (0.245 g, 1.24 mmol) and it was heated at 90°C for more 1.5h with stirring under nitrogen atmosphere. After cooling to rt, the reaction mixture was extracted with chloroform and washed with water. The organic layer was dried over Na₂SO₄ and then evaporated in *vacuo*. The residue was recrystallized from methanol at -20°C. The methanolic layer was removed by filtration. The residue was purified by column chromatography (silica gel,

dichloromethane, Rf = 0.65). After removal of the solvent, 0.307 g of pale yellow solid was obtained. Yield: 61.1%. M.p.: 142.7°C.

R (KBr, cm⁻¹): 2834.62 (-OCH₃), 2226.68 (-CN), 1590.62 (C=C).

¹H-NMR ((D₃C)₂S=O, TMS): δ = 7.45~7.50 (m, 2H, Ar-H), 7.39 (s, 2H, Ar-S-Ar-H), 7.10 (m, 6H, Ar-S-Ar-H), 3.80 (s, 6H, -CH₃).

4,5-Bis(2-methoxyphenylthio)phthalonitrile (10i)

It was purified by column chromatography (silica gel, chloroform : n-hexane = 4 : 1, Rf = 0.50). Yield: 44.0%. M.p.: 192.7°C.

IR (KBr, cm⁻¹): 2836.67 (-OCH₃), 2225.93 (-CN), 1583.07 (C=C).

¹H-NMR ((D₃C)₂S=O, TMS): δ = 7.61~7.56 (m, 2H, Ar-H), 7.47 (dd, 2H, J₁ = 7.8 Hz, J₂ = 1.8 Hz, Ar-S-Ar-H), 7.26 (dd, 2H, J₁ = 8.3 Hz, J₂ = 1.0 Hz, Ar-S-Ar-H), 7.13~7.11 (m, 4H, Ar-S-Ar-H), 3.83 (s, 6H, -CH₃).

4,5-Bis(3,4-dimethoxyphenylthio)phthalonitrile (10k)

It was purified by column chromatography (silica gel, dichloromethane, Rf = 0.13).

Yield: 61.9%. M.p.: 232.7°C.

IR (KBr, cm⁻¹): 2842.58 (-OCH₃), 2227.20 (-CN), 1583.99 (C=C).

¹H-NMR ((D₃C)₂S=O, TMS): δ = 7.21 (dd, 2H, J₁ = 8.3 Hz, J₂ = 2.0 Hz, Ar-H), 7.17~7.15 (m, 4H, Ar-S-Ar-H), 7.11 (s, 2H, Ar-S-Ar-H), 3.85 (s, 6H, -CH₃), 3.80 (s, 6H, -CH₃).

[(m-C₁)PhS]₈PcCu (8j)

A mixture of 4,5-bis(3-methoxyphenylthio)phthalonitrile (**10j**) (0.100 g, 0.247 mmol), 1-hexanol (5 ml) and CuCl₂ (0.0454 g, 0.338 mmol) was refluxed under nitrogen atmosphere for 0.5 h. Then, DBU (5 drops) was added to the reaction mixture and it was refluxed under nitrogen atmosphere for 14 h. After cooling to rt, methanol was poured into the reaction mixture to precipitate the target compound. The methanolic layer was removed by filtration. The residue was washed with methanol, ethanol and acetone successively to afford 0.0604 g of dark green solid was obtained. Yield: 58.2%.

[(o-C₁)PhS]₈PcCu (8i)

Yield: 36.0%.

[(m,p-(C₁)₂)PhS]₈PcCu (8k)

Yield: 19.7%.

MALDI-TOF Mass data for **8i~k**: See Table 1.

Elemental Analysis data for **8h**: See Table 1.

UV-vis spectral data **8i~k**: See Table 2.

Measurements

The Infrared absorption spectra were recorded by using a Nicolet NEXUS670 FT-IR. The ¹H-NMR measurements were carried out by using a Bruker Ultrashield 400 MHz. The elemental analyses were performed by using a Perkin-Elmer Elemental Analyzer 2400. The MALDI-TOF mass spectral measurements were carried out by using a Bruker Daltonics Autoflex III spectrometer (matrix: dithranol). Electronic absorption (UV-vis) spectra were recorded by using a Hitachi U-4100 spectrophotometer. Phase transition behaviour of the present compounds was observed with a polarizing optical microscope (Nikon ECLIPSE E600 POL) equipped with a Mettler FP82HT hot stage and a Mettler FP-90 Central Processor, and a Shimadzu DSC-50 differential scanning calorimeter. The mesophases were identified by using a small angle X-ray diffractometer (Bruker Mac SAXS System) equipped with a temperature-variable sample holder adopted a Mettler FP82HT hot stage. Figs. S1 and S2 illustrate the setup of the SAXS system and the setup of the temperature-variable sample holder, respectively. As can be seen from Fig. S1, the generated X-ray is bent by two

convergence monochrometers to produce point X-ray beam (diameter = 1.0 mm). The point beam runs through holes of the temperature-variable sample holder. As illustrated in Fig. S2, into the temperature-variable sample holder of Mettler FP82HT hot stage, a glass plate (76 mm × 19 mm × 1.0 mm) having a hole (diameter = 1.5 mm) is inserted. The hole can be charged with a powder sample (*ca.* 1 mg). The measurable range is from 3.0 Å to 100 Å and the temperature range is from rt to 375°C. This SAXS system is available for all condensed phases including fluid nematic phase and isotropic liquid.

RESULTS AND DISCUSSION

Synthesis

The compounds synthesized here were characterized by using ¹H-NMR, FT-IR, MALDI-TOF mass spectra (Table 1), elemental analysis (Table 1) and electronic absorption spectra (Table 2). In the elemental analysis, all the present (PhS)₈PcCu derivatives were much less flammable than the long alkyl-chain-substituted (PhO)₈PcCu derivatives. Especially, [(*o*-C₁)PhS]₈PcCu (**8i**) and [(*m*-C₁)PhS]₈PcCu (**8j**) were not completely burnt out so that the observed carbon content showed lower percentage than the calculated value by several percent as the same case of our previous Pc derivatives [17, 23]. Therefore, these data are omitted in this table. This is a well-known characteristic of less flammable phthalocyanine derivatives [24]. However, it could be confirmed from their MALDI-TOF mass spectra in Table 1 and the electronic absorption spectra in Table 2 that the target derivatives 8i~k were surely synthesized.

Electronic absorption spectra

Each of the present PhS-containing derivatives, [(*o*-C₁)PhS]₈PcCu (**8i**), [(*m*-C₁)PhS]₈PcCu (**8j**) and {[*m,p*-(C₁)₂]PhS}₈PcCu (**8k**), showed poor solubility in many solvents. They did not dissolve at all in chloroform, DMF and DMSO. The electronic absorption spectra could not be measured in these solvents. THF gave comparatively better solubility among the other solvents, so that THF was selected as the measurement solvent. Although the solutions were prepared in a very lower concentration at 1.0 × 10⁻⁵ mol/L, a small amount of precipitates were seen in the THF solutions. Hence, the real concentrations were slightly lower than this concentration. In spite of the precipitation, the Q band peak could be clearly detected independently from the small aggregation peak. If strong aggregation would occur, the Q band peak would be covered by the big aggregation band. Thus, the Q band peak could be observed independently from the aggregation band.

In order to investigate the effect of S and O atoms on electronic absorption wavelength, the spectra of our previous PhO-containing derivatives, [(*o*-C₁)PhO]₈PcCu (**7e**), [(*m*-C₁)PhO]₈PcCu (**7f**) and {[*m,p*-(C₁)₂]PhO}₈PcCu (**7g**) [16], were also measured in the same solvent THF. In Table 2 are listed these spectral data as well. As can be seen from this table, the Q bands of the PhS-containing derivatives are located in 709.7 ~ 714.2 nm, which were significantly red-shifted by 34.1 ~ 37.5 nm from the Q bands of the PhO-containing derivatives located in 675.5 ~ 678.0 nm. Q band in Pc derivatives corresponds to the band gap between HOMO and LUMO. Therefore, the PhS group induced a band gap of the HOMO-LUMO narrower than that of PhO group, so that we can expect faster charge carrier mobility for the PhS-substituted PcCu derivatives than that of the PhO-substituted PcCu derivatives. It can be deduced from the analogy between the Pc derivatives substituted by alkylthio group and/or alkoxy group [18]. The charge carrier mobility of the alkylthio-substituted liquid crystal, (C₁₂S)₈PcH₂, is 5 times higher than that of the alkoxy-substituted liquid crystal, (C₁₂O)₈PcH₂ [19].

Phase transition behaviour

Phase transitions of the present flying-seed-like (PhS)₈PcCu derivatives **8i-k** are summarized in Table 3.

As can be seen from this table, when the freshly prepared sample of [(*o*-C₁)PhS]₈PcCu (**8i**) was heated from rt, K₁ crystals relaxed into K₂ crystals at about 180°C. On further heating, the K₂ crystals transformed into K₃ crystals at 301.7°C, and then the K₃ crystals melted into a tetragonal ordered columnar mesophase (Col_{tet.o}) at 314.9°C. The Col_{tet.o} mesophase cleared into isotropic liquid at 362.9°C, accompanied by rapid decomposition.

When the freshly prepared sample of [(*m*-C₁)PhS]₈PcCu (**8j**) was heated from rt, K₁ crystals relaxed into K₂ crystals at about 180°C. On further heating, the K₂ crystals melted into a rectangular ordered columnar mesophase having a P2m symmetry (Col_{ro}(P2m)) at 287.4°C. The Col_{ro}(P2m) mesophase cleared into isotropic liquid at 334.2°C with rapid decomposition. Fig. 2 shows photomicrographs of K₁, K₂ and Col_{ro}(P2m) mesophase together with a DSC thermogram of [(*m*-C₁)PhS]₈PcCu (**8j**) for the 1st heating run at 10°C/min. As can be seen from the photomicrographs in this figure, the freshly prepared (virgin) K₁ crystals were needle-like and the needle-like crystalline shape maintained in the rigid higher temperature K₂ crystals; on the other hand, the Col_{ro}(P2m) mesophase showed stickiness with birefringence when the cover glass plate was pressed. As can be seen from the DSC thermogram in this figure, a big exothermic peak could be observed at *ca.* 180°C as the onset temperature. Since it was not accompanied by a glass transition, the exothermic peak could be assigned as a relaxation directly from K₁ crystals to K₂ crystals. The relaxation and the other phase transitions could be rationally explained by a schematic free energy versus temperature (G-T) diagram illustrated in Fig. 3. When the freshly prepared virgin sample of K₁ crystals is heated from rt. to *ca.* 180°C, the relaxation from line K₁ to line K₂ occurs at an uncertain temperature due to molecular rearrangement which is much easier at the higher temperatures than at rt; on further heating, the resulted K₂ crystals run along the line K₂ to an intersection at 287.4°C, which is the melting point from K₂ to Col_{ro}(P2m). Then, the Col_{ro}(P2m) mesophase runs along the line Col_{ro}(P2m) till another intersection at 334.2°C, which is the clearing point of the Col_{ro}(P2m) mesophase. Thus, the thermal behaviour can be rationally explained by using the G-T diagram.

As can be seen from Table 3, when the freshly prepared sample of {[*m,p*-(C₁)₂]PhS]₈PcCu (**8k**) was heated from rt, it showed not relaxation but a solid-solid (K₁-K₂) phase transition at 267.7°C. On further heating, the K₂ crystals melted into a Col_{ro}(P2m) mesophase at 331.8°C, and the Col_{ro}(P2m) mesophase cleared into isotropic liquid at 386.8°C with rapid decomposition.

Very interestingly, each of the derivatives thus exhibits a columnar mesophase at very high temperatures. The mesomorphism is apparently originated from the novel bulky groups (**i~k**).

Polarizing optical microscopic observation

Fig. 4 shows photomicrographs of the (PhS)₈PcCu derivatives, **8i~k**. Each of the (PhS)₈PcCu derivatives rapidly decomposed just after clearing into isotropic liquid, so that it could not give a natural texture which would be obtained by slow cooling from isotropic liquid. However, as can be seen from the photomicrographs in Fig. 4, each of the derivatives was spread to show stickiness together with birefringence when the cover glass was pressed at the temperature denoted in this figure caption. Stickiness with birefringence is characteristic to mesomorphism. Hence, these states could be identified as mesophases.

These mesophases were fairly stable under nitrogen atmosphere during the DSC measurements, but they were unstable in the air during the POM observations. Fig. 5 shows photomicrographs of the Col_{ro}(P2m) mesophase of {[*m,p*-(C₁)₂]PhS]₈PcCu (**8k**) at 350°C. As can be seen from these photomicrographs, rapid decomposition occurred depending the annealing time. Holding the hot stage at 350°C in advance, the sample between two glass plates was put on the hot stage and pressed to spread. The thin film was immediately observed under a polarizing optical microscope. Fig. 5(a) was a photomicrograph taken immediately after setting on the hot stage. It clearly shows birefringence. After holding it for 3 minutes, the birefringence was losing (Fig. 5(b)), and after 5 minutes, the birefringence completely disappeared (Fig. 5(c)). The birefringence only disappeared without clearing into the isotropic liquid. This means that the birefringence was lost by decomposition. Hence, the present mesophases of (PhS)₈PcCu (**8i~k**) are very unstable in

the air at the high temperatures. We should pay attention on this instability in the air for the temperature-dependent X-ray diffraction measurements.

Temperature-dependent X-ray diffraction measurements

Temperature-dependent small angle X-ray diffraction measurements were carried out by using our originally developed apparatuses illustrated in Figs. S1 and S2. As illustrated in Fig. S2, a liquid crystalline material was filled into a hole of glass plate. As already mentioned above, rapid decomposition of the $\{[m,p-(C_1)_2]PhS\}_8PcCu$ (**8k**) derivative occurred within 5 min at 350°C. Therefore, holding the hot stage at 350 °C in advance, the glass plate filled the liquid crystalline material **8k** in the hole was put on the hot sage. Immediately after the hot stage was set on the hot stage holder illustrated in Fig. S1, the X-ray diffraction measurement was carried out in 5 min, in order to prevent the decomposition in the air as possible as we could. In this case, we could successfully obtain the X-ray diffraction pattern as shown in Fig. 6(c). Therefore, each of X-ray measurements for the $(PhS)_8PcCu$ (**8i-k**) derivatives was carried out in 5 min immediately after the sample insertion. The diffraction patterns of liquid crystal phase and X-ray data were summarized in Fig. 6 and Table 4, respectively.

Fig. 6(a) shows a diffraction pattern of $[(o-C_1)PhS]_8PcCu$ (**8i**) at 340°C. As can be seen from this X-ray diffraction (XRD) pattern, two reflection peaks were observed in the region from $2\Theta = 3^\circ$ to 7° . The spacings of these peaks are exactly in a ratio of 1: $1/\sqrt{2}$ (Table 4), which is characteristic of 2D tetragonal symmetry. Broad halos at $2\Theta = ca.13$ and $ca.24$ may correspond to thermal fluctuations of the phenylthio groups and stacking distance of intracolumnar disks, respectively. Therefore, this mesophase was identified as a $Col_{tet,o}$ mesophase ($a = 20.0 \text{ \AA}$, $h = 3.76 \text{ \AA}$). However, when the number (Z) of molecules in a lattice was calculated from Z Value Calculation [25] by using an assumed density $\rho = 1.0 \text{ g cm}^{-3}$, the Z value was obtained as 0.54. The Z value should be 1.0 for a $Col_{tet,o}$ mesophase. Hereupon, we referred to our previous work on the very similar flying-seed-like mesogen $[(o-C_1)PhO]_8PcCu$ [17] for the stacking distance (h). The previous $[(o-C_1)PhO]_8PcCu$ derivative shows a $Col_{ro}(P2m)$ mesohase having lattice constants, $a = 20.7 \text{ \AA}$, $b = 19.2 \text{ \AA}$ and $h = 7.00 \text{ \AA}$. This $Col_{ro}(P2m)$ mesohase of $[(o-C_1)PhO]_8PcCu$ is very close to the Col_{tet} mesophase of $[(o-C_1)PhS]_8PcCu$, because it has $a \approx b$. Therefore, we thought the stacking distance of the present $[(o-C_1)PhS]_8PcCu$ homologue might be also 7.00 \AA , although this reflection peak was covered by a big halo due to thermal fluctuations of the phenylthio groups (Fig. 6(a)). The stacking distance of 7.00 \AA is very long in comparison with the stacking distances usually observed at 3.5 \AA for conventional tetragonal columnar mesophases, but this stacking distance can be proven as a proper value from Z Value Calculation [25]. The number (Z) of molecules in a lattice can be calculated from this stacking distance ($h = 7.00 \text{ \AA}$) and the lattice constant of 2D tetragonal lattice ($a = 20.0 \text{ \AA}$) listed in Table 4. When ρ , V , N and M are density of mesophase, volume of unite lattice, Avogadro's number and molecular weight, respectively, Z value can be obtained from following equation:

$$\begin{aligned} Z &= (\rho VN)/M = [\rho(a^2 \times h)N]/M \\ &= [1.0(\text{g/cm}^3) \times (20.0 \times 10^{-8} \text{ cm})^2 \times (7.00 \times 10^{-8} \text{ cm}) \times 6.02 \times 10^{23}(\text{/mol})]/1681.57(\text{g/mol}) \\ &= 1.00 \end{aligned}$$

The calculated value $Z = 1.0$ is the same as the theoretical number of molecules in a 2D tetragonal lattice: $Z = 1.0$. Therefore, this big stacking distance $h = 7.00 \text{ \AA}$ is a rationally proper value.

However, a very big peak denoted as X appeared in the very small angle region ($d = 77.3 \text{ \AA}$) could not be assigned as a reflection from any 2D lattices for columnar mesophases known up to date. It may be originated from helicity of columns [26, 27]. At present time, it is not clear and we need further study for this peak.

Fig. 6(b) shows a diffraction pattern of $[(m-C_1)PhS]_8PcCu$ (**8j**) at 300°C. As can be seen from this pattern, the mesophase also gave a very big peak X in the very small angle region ($d = 98.5 \text{ \AA}$). In the region from $2\Theta = 3^\circ$ to 15° , six peaks could be observed. From these peaks, we could identify this mesophase as a $Col_{ro}(P2m)$ mesophase (Table 4).

The lattice constants are $a = 20.7 \text{ \AA}$, $b = 18.1 \text{ \AA}$ and $h = 6.82 \text{ \AA}$. The number (Z) of molecules in a lattice can be obtained from following equation:

$$\begin{aligned} Z &= (\rho VN)/M = [\rho \times (a \times b \times h) \times N]/M \\ &= [1.1(\text{g/cm}^3) \times (20.7 \times 10^{-8} \text{ cm}) \times (18.1 \times 10^{-8} \text{ cm}) \times (6.82 \times 10^{-8} \text{ cm}) \times 6.02 \times 10^{23}(\text{/mol})]/1681.57(\text{g/mol}) \\ &= 1.01 \end{aligned}$$

The calculated value $Z = 1.0$ is the same as the theoretical number of molecules in a 2D rectangular lattice having a P2m symmetry: $Z = 1.0$. Therefore, this stacking distance $h = 6.82 \text{ \AA}$ is a rationally proper value.

Fig. 6(c) shows an XRD pattern of $\{[m,p-(C_1)_2]PhS\}_8PcCu$ (**8k**) at 350°C . As can be seen from this pattern, Peak X did not appear in the very small angle region. It differs from two previous derivatives, **8i** and **8j**. This point may be very helpful to clarify the origin of Peak X in further study. As can be seen also from this XRD pattern, two big peaks appeared closely at around $2\Theta = 4\sim 5^\circ$. This diffraction pattern is often observed for rectangular columnar (Col_r) mesophases. According to our expectation, five peaks were well fitted to a 2D reciprocal rectangular lattice calculated from the lattice constants of $a = 37.1 \text{ \AA}$ and $b = 20.8 \text{ \AA}$, as can be seen from Table 4. Using the stacking distance $h = 3.95 \text{ \AA}$ and an assumed density $\rho = 1.05(\text{g/cm}^3)$, the calculated Z value is 1.0. This value indicates that this mesophase should have a P2m symmetry [25].

The stacking distances of $[(o-C_1)PhS]_8PcCu$ (**8i**) and $[(m-C_1)PhS]_8PcCu$ (**8j**) are 7.00 \AA and 6.82 \AA , respectively, whereas the stacking distance of $\{[m,p-(C_1)_2]PhS\}_8PcCu$ (**8k**) is 3.95 \AA . In our previous work [17], the $(PhO)_8PcCu$ derivatives substituted by mono-methoxy groups tend to show a long stacking distance, $6.09\sim 7.00 \text{ \AA}$, whereas the $(PhO)_8PcCu$ derivatives substituted by multi-methoxy groups tend to show a short stacking distance, $3.87\sim 4.80 \text{ \AA}$. Interestingly, this tendency can be also seen in the present $(PhS)_8PcCu$ derivatives.

Thus, each of the present $(PhS)_8PcCu$ derivatives, **8i-k**, exhibits a columnar mesophase at a very high temperature region. It is very noteworthy that the mesomorphism with a very high temperature region is apparently originated from the novel bulky groups (**i-k**).

CONCLUSION

In this study, we have synthesized three novel flying-seed-like liquid crystals based on $(PhS)_8PcCu$: $[(m-C_1)PhS]_8PcCu$ (**8i**), $[(o-C_1)PhS]_8PcCu$ (**8j**) and $\{[m,p-(C_1)_2]PhS\}_8PcCu$ (**8k**), to investigate their mesomorphism. As the results, each of the derivatives exhibits a columnar mesophase at very high temperatures: **8i** $Col_{et.o}$ at $314.9 \sim 362.9^\circ\text{C}$ for **8i**, $Col_{r0}(P2m)$ at $287.4 \sim 334.2^\circ\text{C}$ for **8j** and $Col_{r0}(P2m)$ at $331.8 \sim 386.8^\circ\text{C}$ for **8k**. Very interestingly, the mesomorphism is apparently originated from the novel bulky groups (**i-k**). The Q bands of the present PhS-containing Pc derivatives **8i-k** significantly red-shift by about 35nm in comparison with those of the corresponding PhO-containing derivatives **7e**, **7f** and **7h**. Since the Q band in Pc derivatives corresponds to the band gap between HOMO and LUMO, the charge carrier mobilities may be greatly improved by the substitution of PhS instead of PhO. Each of them rapidly decomposed after clearing into isotropic liquid. On the other hand, these high temperature mesophases were fairly stable under nitrogen atmosphere but they were unstable in the air. Thus, the present flying-seed-like liquid crystals based on $(PhS)_8PcCu$ are unfortunately unstable at higher temperatures in the air. If the thermal instability will be improved by chemical modification, fast charge carrier mobilities will be realized for the $(PhS)_8PcCu$ -based derivatives in the future. There are still a very few examples of flying-seed-like liquid crystals. Therefore, we believe that this work will contribute to the development of a new research field of the flying-seed-like liquid crystals.

REFERENCES

1. Keller H. *Mol. Cryst. Liq. Cryst.* 1973; **21**: 1-48.

2. V. Vill *Condensed Matter News* 1992; **1**: 25-28.
3. Chandrasekhar S, Sadashiva BK, Suresh KA. *Pramana*, 1977; **9**: 471-480.
4. Vorländer D. *Ber.*, 1911; **43**: 3120-3125.
5. Demus D, Sackmann H, Seibert K. *Wiss. Z. Univ. Halle, Math.-Nat. R.* 1970; **19**: 47-62.
6. Ferloni P, Sanesi M, Tonelli PL, Franzosini P. *Z. Naturforsch.* 1978; **33a**: 240-242.
7. Sanesi M, Ferloni P, Spinolo G, Tonelli PL. *Z. Naturforsch.* 1978; **33a**: 386-388.
8. van Deun R, Ramaekers J, Nockemann P, van Hecke K, van Meervelt L, Binnemans K. *Eur. J. Inorg. Chem.*, 2005; 563-571.
9. Ohta K, Shibuya T, Ando M, *J. Mater. Chem.*, 2006; **16**: 3635-3639.
10. Basurto S, Garcia S, Neo AG, Torroba T, Marcos CF, Miguel D, Barbera J, Ros MB, de la Fuente MR. *Chem. Eur. J.*, 2005; **11**: 5362-5376.
11. Shimizu M, Nata M, Watanabe K, Hiyama T, Ujiie S. *Mol. Cryst. Liq. Cryst.*, 2005; **441**: 237-241.
12. Shimizu M, Nata M, Mochida K, Hiyama T, Ujiie S, Yoshio M, Kato T, *Angew. Chem. Int. Ed.*, 2007; **46**: 3055-3058.
13. Usol'tseva N, Bykova V, Ananjeva G, Zharnikova N. *Mol. Cryst. Liq. Cryst.* 2004; **411**: 1371-1378.
14. Zharnikova N, Usol'tseva N, Kudrik E, Theakkat M. *J. Mater. Chem.*, 2009; **19**: 3161-3167.
15. Takagi Y, Ohta K, Shimosuigi S, Fujii T, Itoh E. *J. Mater. Chem.*, 2012; **22**: 14418-14425.
16. Hachisuga A, Yoshioka M, Ohta K, Itaya T. *J. Mater. Chem. C*, 2013; **1**: 5315-5321.
17. Yoshioka M, Ohta K, Yasutake M. *RSC Advances*, 2015, **5**, 13828-13839.
18. Ban K, Nishizawa K, Ohta K, Shirai H. *J. Mater. Chem.*, 2000; **10**: 1083-1090.
19. van de Craats M, Schouten PG, Warman JM. *EKISHO*, 1998; Vol. 2, No.1 and the references cited therein.
20. Balakireva OV, Maizlish VE, Shaposhnikov GP. *Russian Journal of General Chemistry*, 2003; **73**: 292-296.
21. Arican D, Arici M, Ugur AL, Erdogmus A, Koca A. *Electrochimica Acta*, 2013; **106**: 541-555.
22. Wohrle D, Eskes M, Shigehara K, Yamada A. *Synthesis*, 1993; 194-196.
23. Shimizu M, Tauchi L, Nakagaki T, Ishikawa A, Itoh E, Ohta K. *J. Porphyrins Phthalocyanines*, 2013; **17**: 264-282.
24. van der Pol JF, Neeleman E, van Miltenburg JC, Zwikker JW, Nolte RJM, Drenth W. *Macromolecules*, 1990; **23**: 155-162.
25. Ohta K. "Dimensionality and Hierarchy of Liquid Crystalline Phases: X-ray Structural Analysis of the Dimensional Assemblies", Shinshu University Institutional Repository, submitted on 11 May, 2013; <http://hdl.handle.net/10091/17016>; Ohta K. "Identification of discotic mesophases by X-ray structure analysis," in "Introduction to Experiments in Liquid Crystal Science (Ekisho Kagaku Jikken Nyumon [in Japanese])" ed., Japanese Liquid Crystal Society, Chapter 2-(3), pp. 11-21, Sigma Shuppan, Tokyo, 2007; ISBN-13: 978-4915666490.
26. Tauchi L, Nakagaki T, Shimizu M, Itoh E, Yasutake M, Ohta K. *J. Porphyrins Phthalocyanines*, 2013; **17**: 1080-1093.
27. Ishikawa A, Ono K, Ohta K, Yasutake M, Ichikawa M, Itoh E., *J. Porphyrins Phthalocyanines*, 2014; **18**: 366-379.

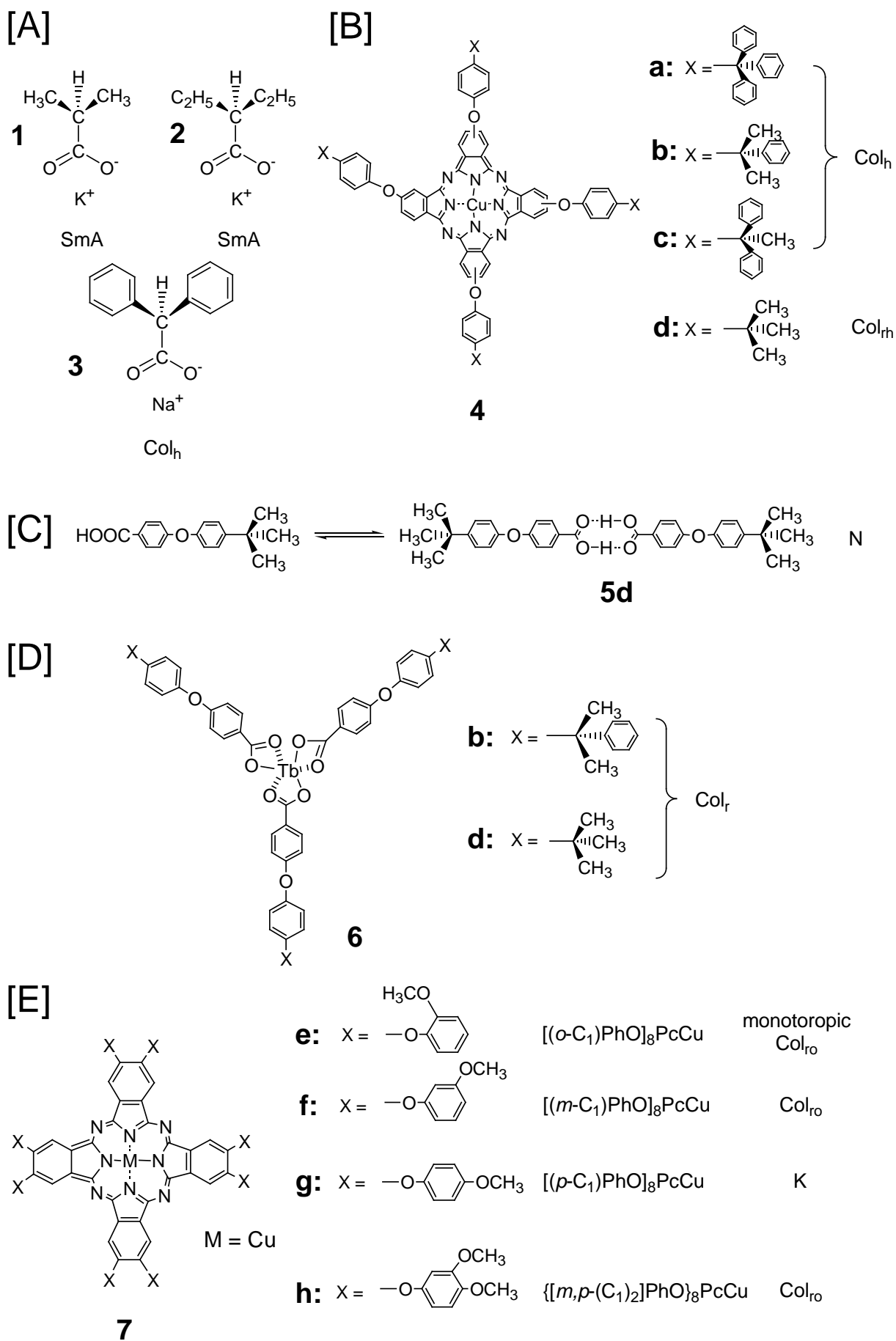
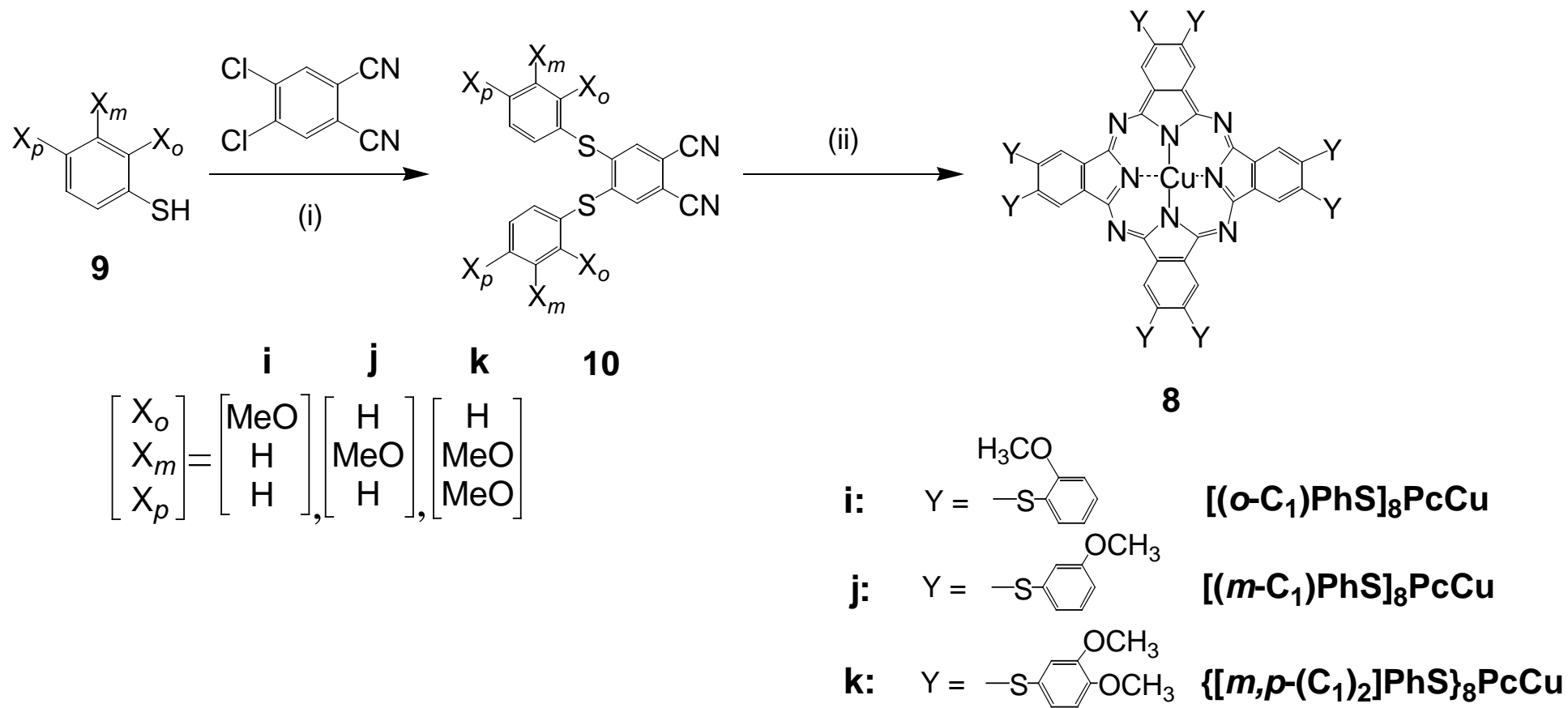


Fig. 1. Flying-seed-like liquid crystals synthesized to date.



Scheme 1. Synthetic route for the flying-seed-like compounds, **8i-k**: (i) K₂CO₃, DMSO, (ii) CuCl₂, DBU, 1-hexanol. DMSO = dimethylsulfoxide and DBU = 1,8-diazabicyclo[5,4,0]-undec-7-ene.

Table 1 . Yields, MALDI-TOF mass spectral data and elemental analysis data of **8i-k**.

Compound	Yield (%)	Mol. formula (Exact Mass)	Observed Mass	Mol. formula (Average Mass)	Element analysis; found(%) (calculated %)		
					C	H	N
8i: [(<i>o</i> -C ₁)PhS] ₈ PcCu	36.0	C ₈₈ H ₆₄ N ₈ O ₈ S ₈ Cu (1679.19)	1679.14	C ₈₈ H ₆₄ N ₈ O ₈ S ₈ Cu (1681.57)	-	-	-
8j: [(<i>m</i> -C ₁)PhS] ₈ PcCu	58.2	C ₈₈ H ₆₄ N ₈ O ₈ S ₈ Cu (1679.19)	1679.22	C ₈₈ H ₆₄ N ₈ O ₈ S ₈ Cu (1681.57)	-	-	-
8k: {[<i>m,p</i> -(C ₁) ₂]PhS} ₈ PcCu	19.7	C ₉₆ H ₈₀ N ₈ O ₁₆ S ₈ Cu (1919.28)	1919.23	C ₉₆ H ₈₀ N ₈ O ₁₆ S ₈ Cu (1921.78)	60.15 (60.00)	3.72(4.20)	6.01 (5.83)

–: This compound did not completely burn out so that the observed carbon content showed lower by several percent than the calculated values. Therefore, these elemental analysis data are omitted here.

Table 2. UV-vis spectral data in THF of the present (PhS)₈PcCu derivatives **8i-k** and the previous (PhO)₈PcCu derivatives **7e,f,h**.

Compound	Concentration [#] (X10 ⁻⁵ mol/l)	λ_{\max} (nm) (log ϵ)				
		Soret-band		Q ₀₋₁ band	Q-band	
					*	Q ₀₋₀ band
8i: [(o-C₁)PhS]₈PcCu	1.0 [‡]	288.2 (4.32)	352.8 (4.32)	645.1 (4.17)	669.6 (sh)	714.2 (4.51)
8j: [(m-C₁)PhS]₈PcCu	1.0 ^{‡□}	288.2 (4.29)	354.7 (4.29)	637.3 (4.11)	678.7 (sh)	709.7 (4.54)
8k: {[m,p-(C₁)₂]PhS}₈PcCu	0.99 ^{‡Z}	290.7 (4.49)	352.8 (4.49)	639.9 (4.27)	677.4 (sh)	712.1 (4.62)

7e: [(o-C₁)PhO]₈PcCu[†]	1.0	279.1 (4.88)	348.3 (4.96)	608.8 (4.68)	646.3 (sh)	676.7 (5.44)
7f: [(m-C₁)PhO]₈PcCu[†]	1.0	283.1 (4.86)	350.6 (4.92)	609.3 (4.64)	645.5 (sh)	675.5 (5.39)
7h: {[m,p-(C₁)₂]PhO}₈PcCu[†]	1.0	288.7 (4.63)	347.1 (4.63)	611.1 (4.38)	647.8 (sh)	678.0 (5.03)

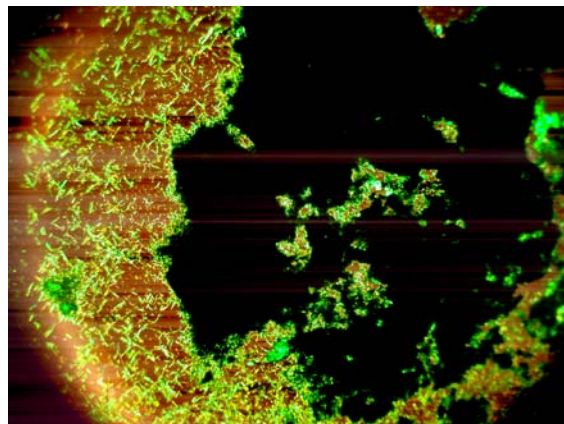
#: In THF. *:Aggregation band of Q₀₋₀ band. sh: Shoulder. ‡:: Although the THF solution was prepared at this concentration, precipitation occurred to some extent. Hence, the real concentration is lower than this concentration. †:: Ref. [17]

Table 3. Phase transition temperatures and enthalpy changes of **8i-k**.

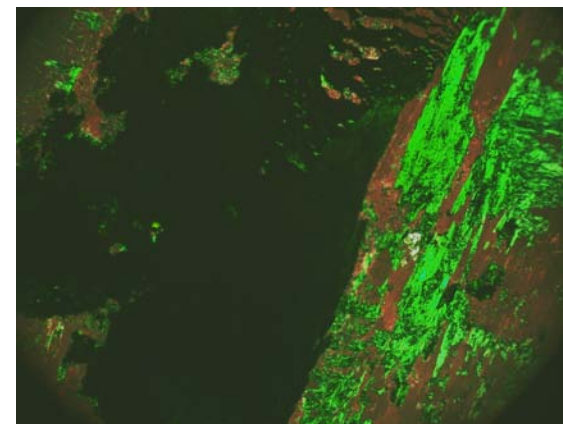
Compound	Phase	$T/^{\circ}\text{C}$ [$\Delta\text{H}(\text{kJmol}^{-1})$]		Phase
8i: [(<i>o</i>-C₁)PhS]₈PcCu	K ₁			
	ca. 180	301.7 [50.1]	314.9 [7.77]	Col _{tet.o}
8j: [(<i>m</i>-C₁)PhS]₈PcCu	K ₁			
	ca. 180	287.4 [3.78]	334.2 [6.72]	Col _{ro} (P2m)
8k: {[<i>m,p</i>-(C₁)₂]PhS}₈PcCu	K ₁			
		267.7 [1.84]	331.8 [34.0]	Col _{ro} (P2m)
			386.8 [3.23]	I.L. (decomp.)



K_1 at r.t. (needle-like crystals)



K_2 at 250°C (rigid)



$Col_{ro}(P2m)$ at 300°C (sticky)

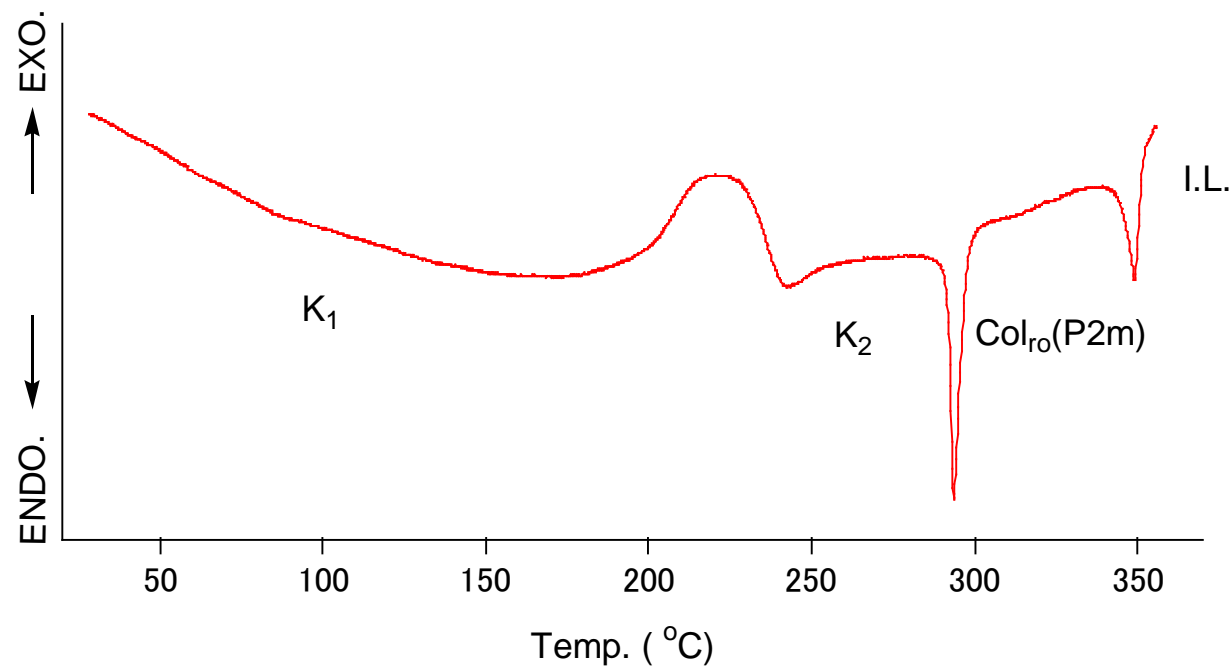


Fig. 2. Photomicrographs of K_1 , K_2 and Col_{ho} mesophase and DSC thermogram of $[(m-C_1)PhS]_8PcCu$ (**8j**) for the 1st heating run at 10°C/min.

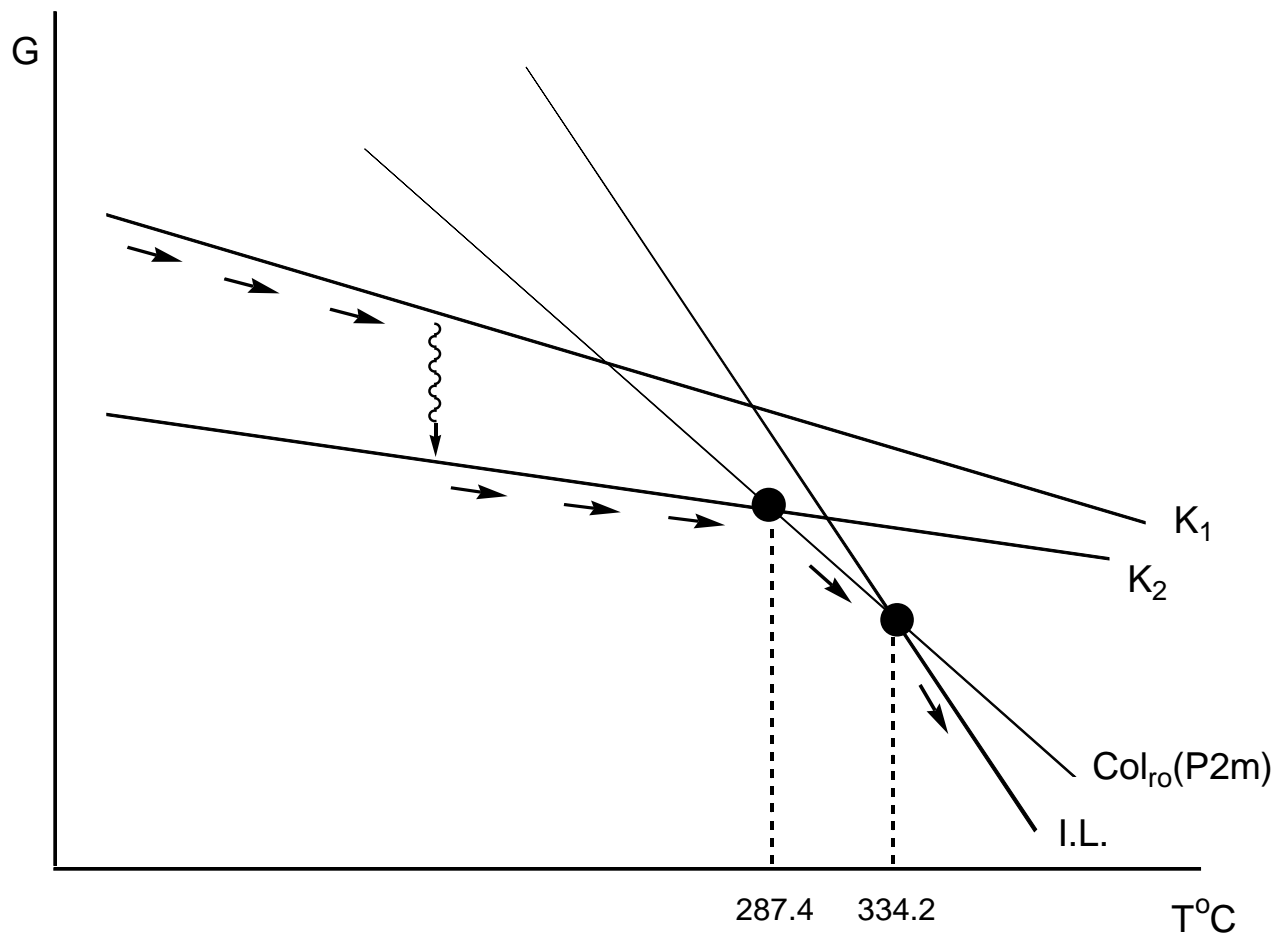


Fig. 3. A schematic G-T diagram of $[(m-C_1)PhS]_8PcCu$ (8j).

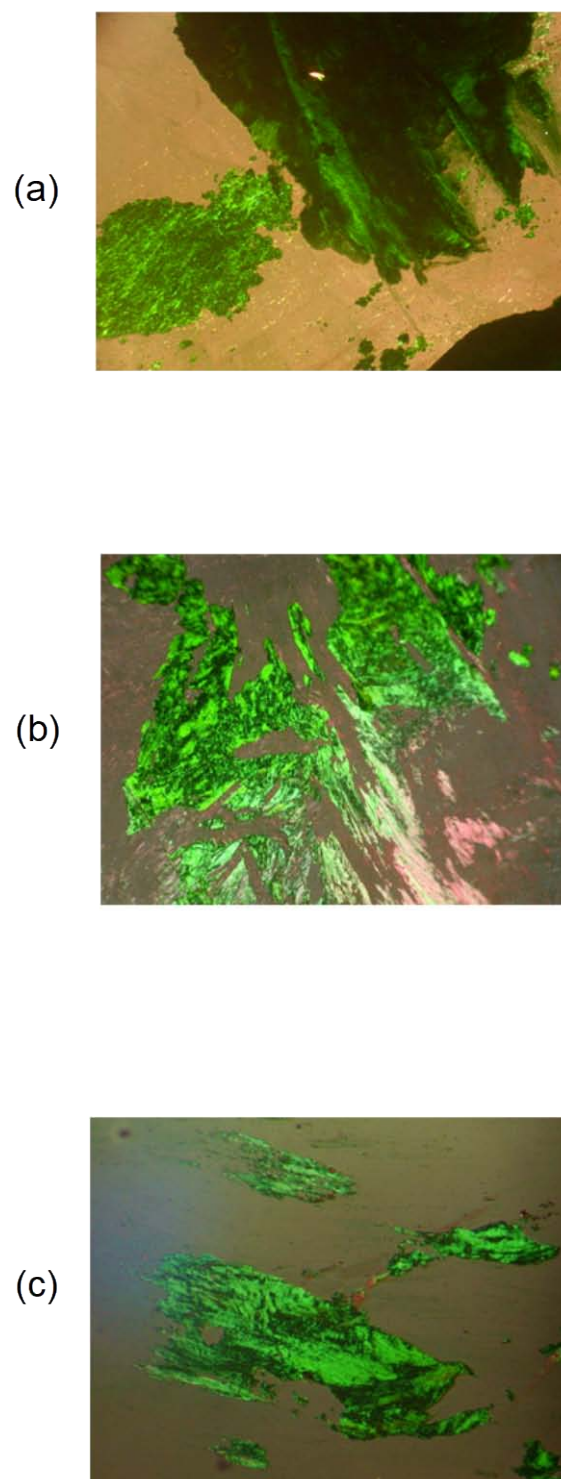


Fig. 4. Photomicrographs of the mesophases of **8i-k**: (a) **8i**: $[(o-C_1)PhS]_8PcCu$ at $330^\circ C$, (b) **8j**: $[(m-C_1)PhS]_8PcCu$ at $300^\circ C$, and (c) **8k**: $\{[m,p-(C_1)_2]PhS\}_8PcCu$ at $350^\circ C$.

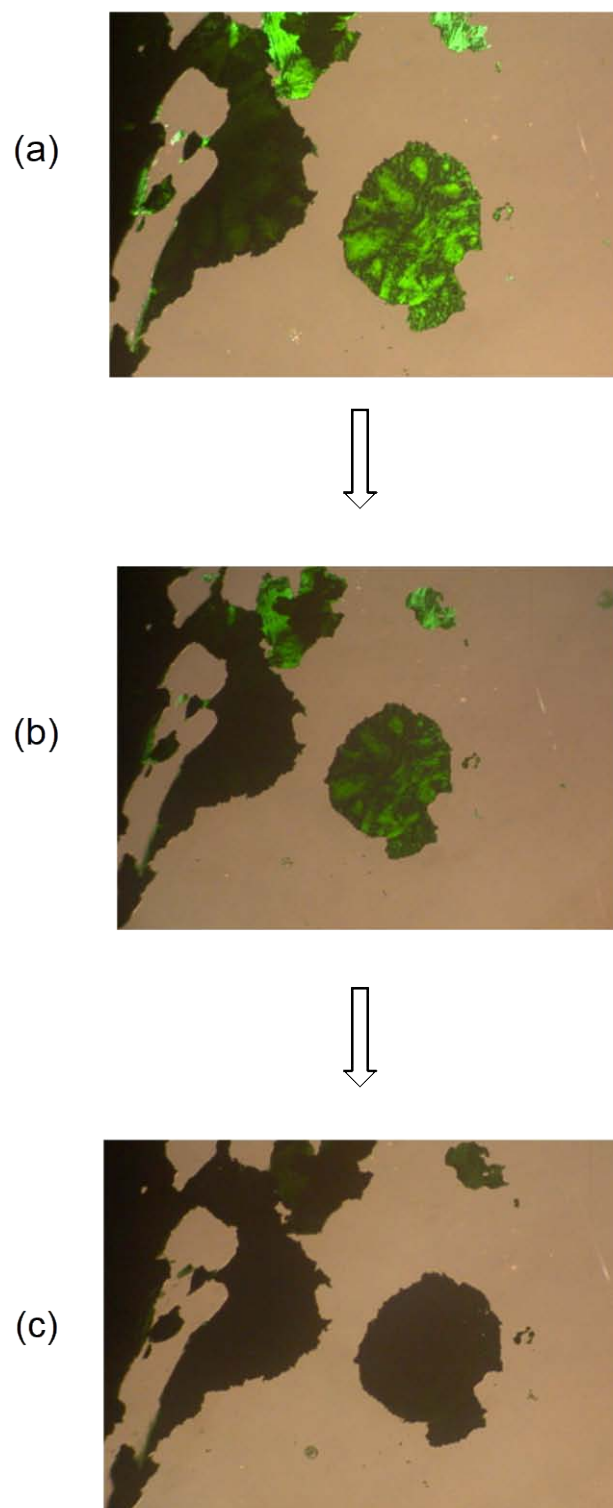
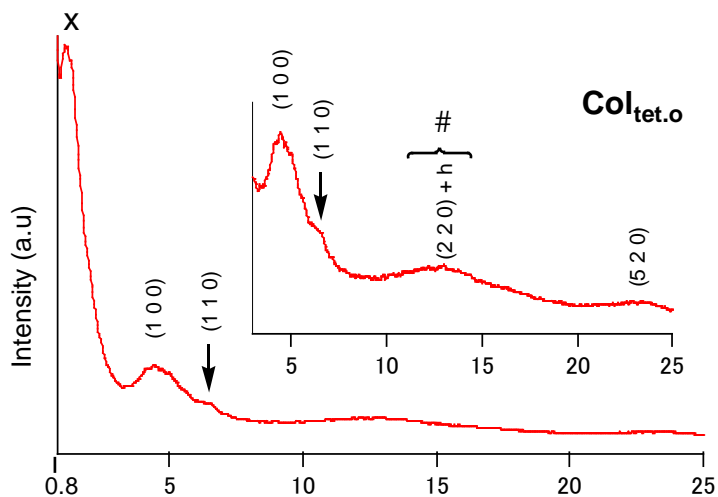
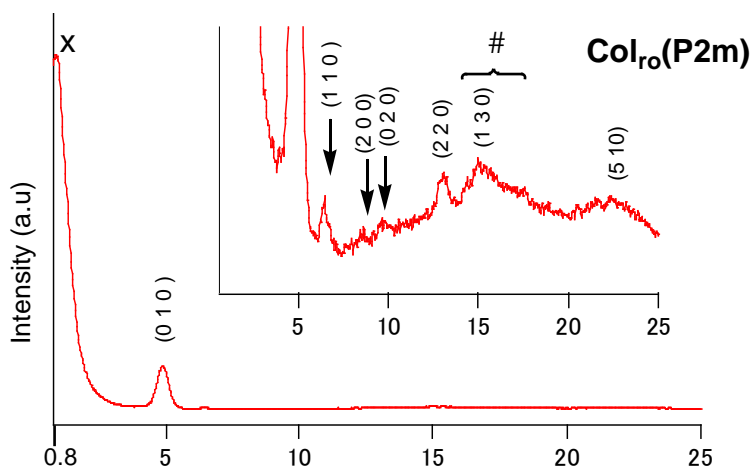


Fig. 5. Annealing-time-dependent birefringence of $\{[m,p\text{-}(C_1)_2]\text{PhS}\}_8\text{PcCu}$ (**8k**) at 350°C : (a) for 0 min , (b) for 3 min , and (c) for 5 min.

(a) **8i**: $[(o-C_1)PhS]_8PcCu$



(b) **8j**: $[(m-C_1)PhS]_8PcCu$



(c) **8k**: $\{[m,p-(C_1)_2]PhS\}_8PcCu$

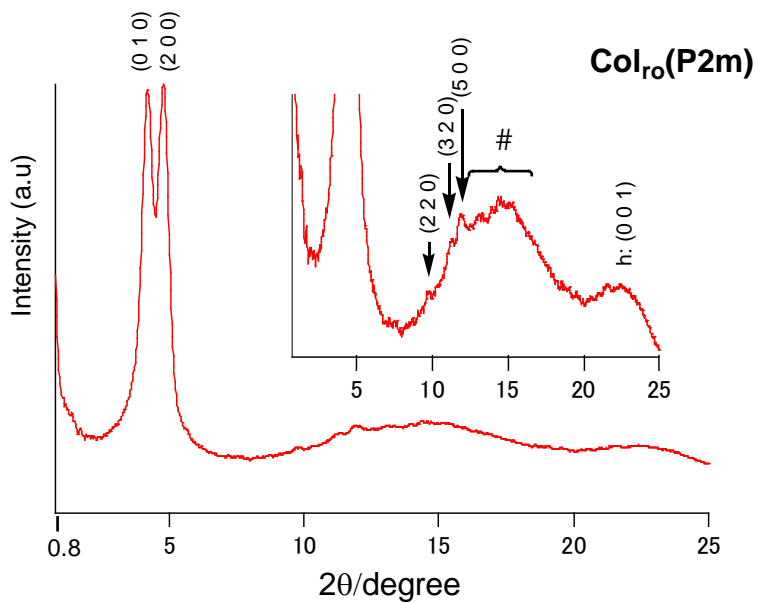


Fig. 6. Small angle X-ray diffraction patterns: (a) **8i** at 340°C, (b) **8j** at 300°C and (c) **8k** at 350°C.

Table 4. X-ray data of **8i-k**.

Compound [mesophase]	Lattice constants/Å	Spacing/Å		Miller indices
		Observed	Calculated	(<i>h k l</i>)
8i: [(o-C₁)PhS]₈PcCu [Col _{tet.o} at 340°C]		77.3	-	X
	a = 20.0	20.0	20.0	(1 0 0)
	h = 7.00	14.1	14.1	(1 1 0)
	Z = 1.0 for ρ = 1.0	ca.7.00	7.04	(2 2 0) + <i>h</i> + #
		3.76	3.71	(5 2 0)
8j: [(m-C₁)PhS]₈PcCu [Col _{r0} (P2m) at 300°C]		98.5	-	X
	a = 20.7 b = 18.1	18.1	18.1	(0 1 0)
	h = 6.82	13.6	13.6	(1 1 0)
	Z = 1.0 for ρ = 1.1	10.1	10.3	(2 0 0)
		9.16	9.05	(0 2 0)
		6.82	6.81	(2 2 0) + <i>h</i>
		ca.5.91	5.79	(1 3 0) + #
		3.98	4.03	(5 1 0)
8k: {[m,p-(C₁)₂]PhS}₈PcCu [Col _{r0} (P2m) at 350°C]		21.0	21.0	(0 1 0)
	a = 37.1 b = 20.8	18.4	18.4	(2 0 0)
	h = 3.95	9.04	9.07	(2 2 0)
	Z = 1.0 for ρ = 1.05	7.83	7.83	(3 2 0)
		7.43	7.43	(5 0 0)
		ca. 5.94	-	#
		3.95	-	<i>h</i>

h: Stacking distance = (0 0 1). #: Broad halo due to thermal fluctuation of the phenylthio groups. X: Reflection unable to be assigned. ρ: Assumed density (g/cm³).

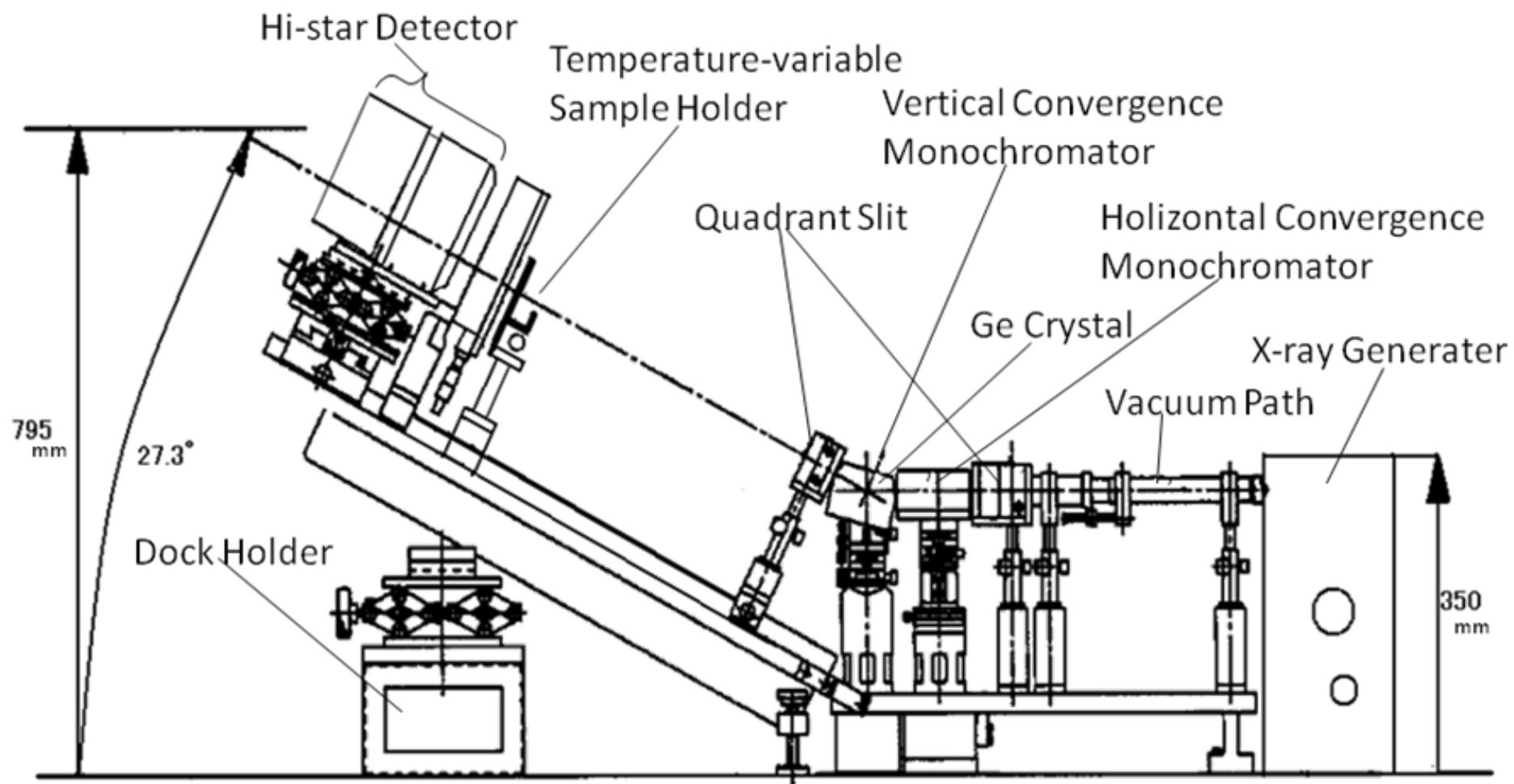
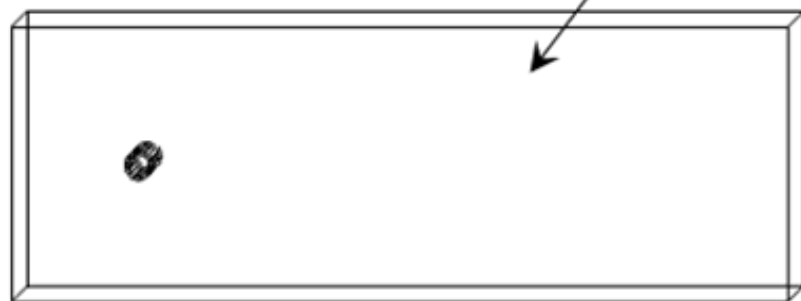
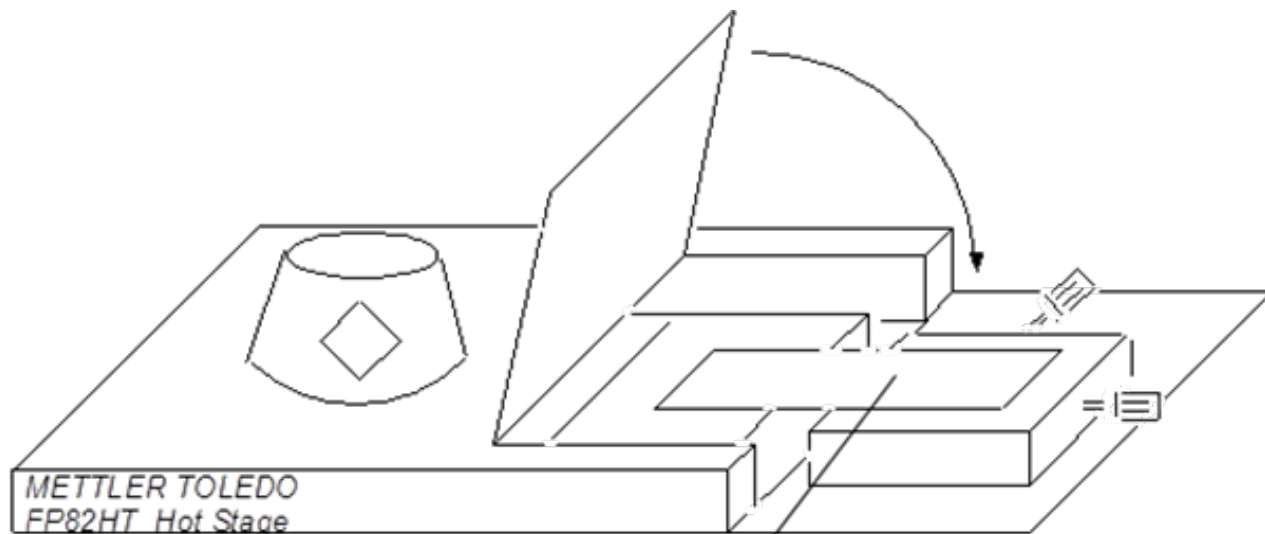


Fig. S1. Setup of Small-Angle X-ray Scattering (Bruker MAC SAXS) equipped with a temperature-variable sample holder.



Measurable range

- Spacing : 3 ~ 100 Å
- Temperature : rt. ~ 375 °C
- Phase : crystals, mesophases, and isotropic liquid.

(*Available for fluid nematic phase and isotropic liquid)

Fig. S2. Setup of the temperature-variable sample holder.